NASA TECHNICAL NOTE

NASA TN D-7673

NASA TN D-7673

CREEP BEHAVIOR OF TANTALUM ALLOY T-222 AT 1365 TO 1700 K

by Robert H. Titran

Lewis Research Center
Cleveland, Ohio 44135

NATIONAL AERONAUTICS AND SPACE ADMINISTRATION • WASHINGTON, D. C. • JUNE 1974

1. Report No.	2. Government Accession No.	3. Recipient's Catalog No.
NASA TN D-7673		

4. Title and Subtitle	5. Report Date
CREEP BEHAVIOR OF TANTALUM ALLOY T-222 AT 1365 TO 1700 K	June 1974
	6. Performing Organization Code
7. Author(s)	8. Performing Organization Report No.
Robert H. Titran	E-7790
	10. Work Unit No.
9. Performing Organization Name and Address	501-21
Lewis Research Center National Aeronautics and Space Administration Cleveland, Ohio 44135	11. Contract or Grant No.
	13. Type of Report and Period Covered
12. Sponsoring Agency Name and Address	Technical Note
National Aeronautics and Space Administration Washington, D.C. 20546	14. Sponsoring Agency Code

15. Supplementary Notes

16. Abstract

High vacuum creep tests on the tantalum T-222 alloy at 0.42 to 0.52 T_m show that the major portion of the creep curves, up to at least 1 percent strain, can be best described by an increasing creep rate, with strain varying linearly with time$^{3/2}$. Correlation and extrapolation of the creep curves on the basis of increasing creep rates results in more accurate engineering design data than would use of approximated linear rates. Based on increasing creep rates, the stress for 1 percent strain in 10 000 hours for T-222 is about four times greater than for the Ta-10W alloy. Increasing the grain size results in increased creep strength. Thermal aging prior to testing caused precipitation of the hexagonal close packed $(Hf, Ta)_2C$, which initially increased creep strength. However, this dimetal carbide was converted during creep testing to face-centered cubic (Hf, Ta)C.

17. Key Words (Suggested by Author(s))	18. Distribution Statement
Tantalum alloys; Creep; Grain size; Temperature dependency; Stress dependency; Precipitation strengthened; Deformation mechanism; Grain boundary sliding	Unclassified - unlimited Category 17

19. Security Classif. (of this report)	20. Security Classif. (of this page)	21. No. of Pages	22. Price*
Unclassified	Unclassified	33	$3.25

* For sale by the National Technical Information Service, Springfield, Virginia 22151

CONTENTS

CREEP BEHAVIOR OF TANTALUM ALLOY T-222 AT 1365 TO 1700 K

by Robert H. Titran

Lewis Research Center

SUMMARY

A study of the kinetics and structural dependence of creep of the tantalum T-222 alloy in the 1365 to 1700 K (0.42 to 0.52 T_m) temperature range was conducted. At low stress levels and long times, creep is best described by an increasing creep rate where creep strain varies linearly with time$^{3/2}$. Creep is believed to be controlled by dislocation climb adjacent to grain boundaries which accommodates grain boundary sliding. The increasing creep rate is believed to be early tertiary creep which is promoted by the nucleation of cavities at grain boundary particles during grain boundary sliding.

The creep strength of T-222 is enhanced by the presence of carbide particles. The apparent activation for tertiary creep ΔH_c was found to be 545 kJ/g-mol, substantially higher than that observed (378 kJ/g-mol) for the single-phase Ta-10W alloy. The high value of ΔH_c observed for T-222 suggests that dislocation motion is impeded by strain-induced carbide precipitation. For comparable grain sizes, the exponential stress-dependency of the tertiary creep rate for the particle strengthened T-222 was 2.33, while Ta-10W exhibited a dependency of about 1.75. The tertiary creep data show a strong correlation to Langdon's creep model. The T-222 alloy showed a change in the exponential stress-dependency of the tertiary creep rate with applied stress, 2.33 at low stress levels (below about 80 MN/m^2) and 4.74 at the higher stress levels studied.

Thermal aging prior to creep testing enhanced creep strength through precipitation of the hexagonal close packed (hcp) dimetal carbide (Hf, Ta)$_2$C. However, during creep testing, the (Hf, Ta)$_2$C was converted to the face-centered cubic (fcc) monocarbide (Hf, Ta)C. In tests of 5 to 1000 hours, only the monocarbide was found and it appears to be the equilibrium phase in the presence of strain.

Extrapolation of the creep curves to obtain the stress levels for 1 percent strain in 10 000 hours showed that T-222 would have a stress capability of approximately 20 MN/m^2 at 1480 K but only 2 MN/m^2 at 1700 K. These strength levels are approximately four times greater than those of the Ta-10W alloy under similar conditions.

INTRODUCTION

Tantalum base alloys have received considerable attention during the past decade, primarily for high temperature structural applications in space power systems. These alloys include tantalum - 10 tungsten (Ta-10W), T-111 (tantalum - 8 tungsten - 2 hafnium), T-222 (tantalum - 9.6 tungsten - 2.4 hafnium - 0.01 carbon), and Astar 811C (tantalum - 8 tungsten - 1 rhenium - 0.7 hafnium - 0.025 carbon). The intended applications would require these materials to operate at temperatures of 1000 to 1900 K (0.3 to 0.6 T_m) for periods of 10 000 to 50 000 hours. Under these conditions, creep resistance of the material becomes a major design consideration.

During previous long-time creep evaluations of tantalum and columbium alloys (refs. 1 to 6), several features of the creep behavior were observed which merited further attention. These features were, first, a strong dependence of creep rate on grain size, with coarse grained materials exhibiting lower creep rates than fine grained materials. Second, a continually increasing creep rate as a function of time starting at total strains of generally less than 0.25 percent was noted. Third, the carbon-containing alloys exhibited lower creep rates than noncarbon-containing alloys when evaluated at comparable grain sizes and test conditions.

The purpose of the present study was to better define the long time high vacuum creep behavior of T-222. This study was concerned with determining whether or not T-222 exhibits similar grain size effects and accelerating creep as noted previously in Ta-10W (ref. 1). It was also of interest to determine the creep strength of T-222 over the temperature range 1365 to 1700 K and the role of carbide particles on the creep behavior. To this end, previously published data by this author were reevaluated and new data were obtained on the effects of grain size and aging treatments.

SYMBOLS

The units for physical quantities used in this report are given in the International System of Units (SI); however, measurements during the investigation were made in U. S. customary units. Factors relating these two systems of units are given in the appendix.

a, b, c	coefficients of polynomials
ΔH_c	apparent activation energy for creep, J/g-mol
ΔH_{sd}	activation energy for lattice self diffusion, J/g-mol
K, K^1	constant

L average grain size, μm

n exponential stress dependency of creep rate

R gas constant, 8.314×10^3 J/(g-mol)(K)

T temperature, K

T_m melting point, 3268 K

$\dot{\alpha}$ primary creep rate, $(\text{strain}^2)(\text{sec}^{-1})$

$\dot{\beta}$ tertiary creep rate, $(\text{strain}^{2/3})(\text{sec}^{-1})$

ϵ creep strain

ϵ_{gb} creep strain due to grain boundary sliding

ϵ_o creep strain on loading

$\dot{\epsilon}_s$ secondary creep rate, sec^{-1}

σ engineering stress, MN/m^2

MATERIALS AND PROCEDURES

The materials used in this study were 0.076- and 0.102-centimeter-thick T-222 alloy sheets. Each thickness was from separate heats procured commercially. The manufacturer reported that the material had been cold-rolled 85 to 90 percent following the last in-process anneal. Prior to shipping, heat A was further vacuum annealed for 2 hours at 1590 K and heat B was vacuum annealed for 2 hours at 1755 K. Chemical analyses of the two heats are shown in table I.

TABLE I. - CHEMICAL ANALYSES OF T-222

Heat	Composition, wt. %						
	Tantalum	Tungsten	Hafnium	Carbon	Oxygen	Nitrogen	Hydrogen
A	Balance	9.11	1.91	0.0113	0.0045	0.0014	0.0002
B	Balance	10.17	2.71	.0101	.0080	.0009	.0005

Creep specimens with a reduced gage section of 2.54 by 0.635 centimeters, as shown in figure 1, were machined from sheet with the specimen axis parallel to the final rolling direction. These specimens were washed in distilled water, degreased in alcohol, wrapped in cleaned tantalum foil, and annealed in a titanium sputter ion pumped furnace at a pressure of less than 10^{-5} N/m^2. Annealing temperatures ranged from

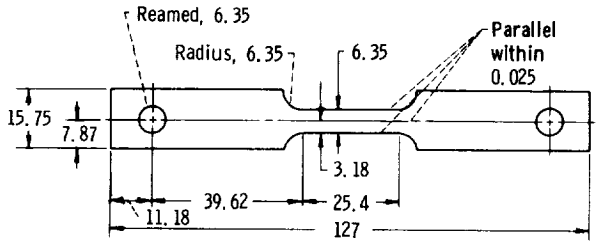

Figure 1. - Standard sheet creep test specimen. Tensile axis parallel to final rolling direction. (All dimensions are given in mm.)

1700 to 2250 K in order to provide materials with different grain sizes. Temperatures were measured with a tungsten/tungsten - 26 percent rhenium thermocouple and are estimated to be accurate within 5 K.

All creep specimens were weighed to the nearest 0.1 milligram before and after annealing to determine if contamination resulted during heat treatment. In all cases, no significant weight changes were observed, indicating that the possible contamination amounted to less than 10 ppm by weight. The annealing schedules resulted in specimens with initial average grain sizes ranging from 16 to 250 micrometers. Grain sizes were also determined after creep testing; these final grain sizes were used in correlating grain size effects. The average grain diameters were determined by counting the number of boundary intercepts with a measured circle on a projection screen.

The titanium-sputter ion pumped, high vacuum (10^{-7}-N/m^2) creep facilities used in this study are described in detail in references 2 and 3. Creep strain measurements were performed optically. A cathetometer clamped to the furnace chamber frame was used to sight on Knoop hardness impressions placed 2.54 centimeters apart on the reduced section of each specimen. The precision of creep-strain measurements is estimated to be ±0.02 percent for the gage length used. In all instances, an initial gage length was read at the test temperature prior to loading of the specimen. The strain on loading was measured and is incorporated in the reported creep strain. Creep testing was usually terminated after a total creep strain of 2 to 3 percent.

Post-test examination included chemical analysis for possible oxygen contamination during testing and metallographic examination for grain size, void and/or crack formation. Scanning electron microscopy and carbon replication were employed for detailed studies of the microstructure. X-ray analysis was employed to identify bromine-extracted particles.

RESULTS AND DISCUSSION

Time Dependence of Creep

Typical creep curves from reference 2 for fine grained T-222 (heat A) tested at 1365, 1480, 1590, and 1700 K are shown in figure 2. These curves show a small strain on loading ϵ_o and a very short period of primary and secondary creep followed by a period of accelerating creep rate at total strains of less than 1 percent. This early onset of an accelerating creep rate was studied earlier on the single-phase Ta-10W alloy (ref. 1). It was shown that the concave upward creep curves could be expressed by a polynomial of the form

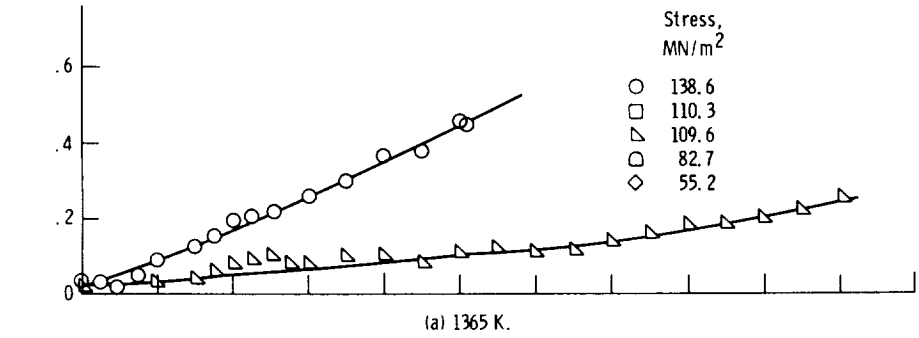

(a) 1365 K.

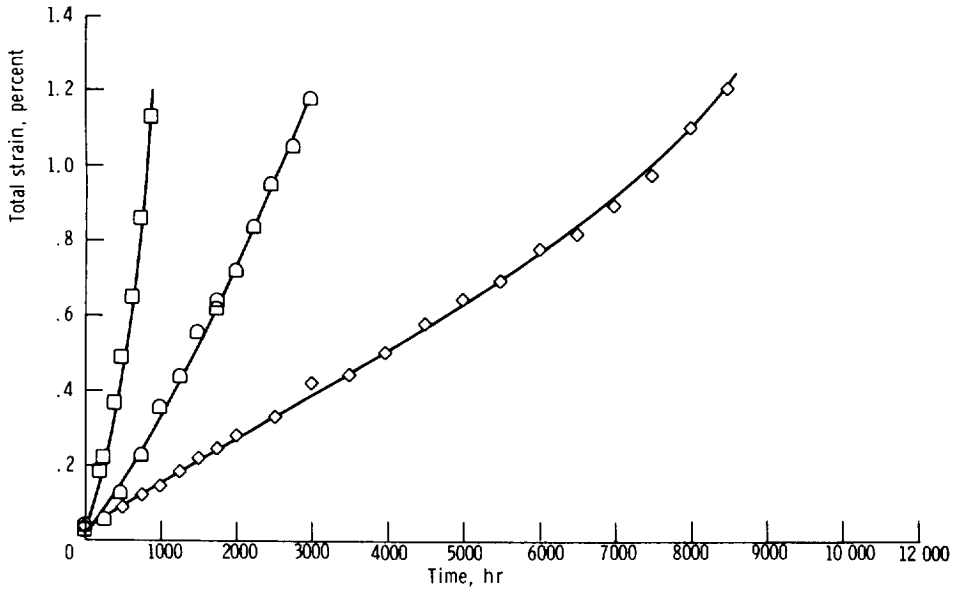

(b) 1480 K.

Figure 2. - Creep curves for T-222 alloy (heat A) illustrating accelerating creep. All specimens annealed for 1 hour at 1810 K prior to creep testing at indicated temperatures and stresses. Grain size, 16 micrometers. (Creep data from ref. 2.)

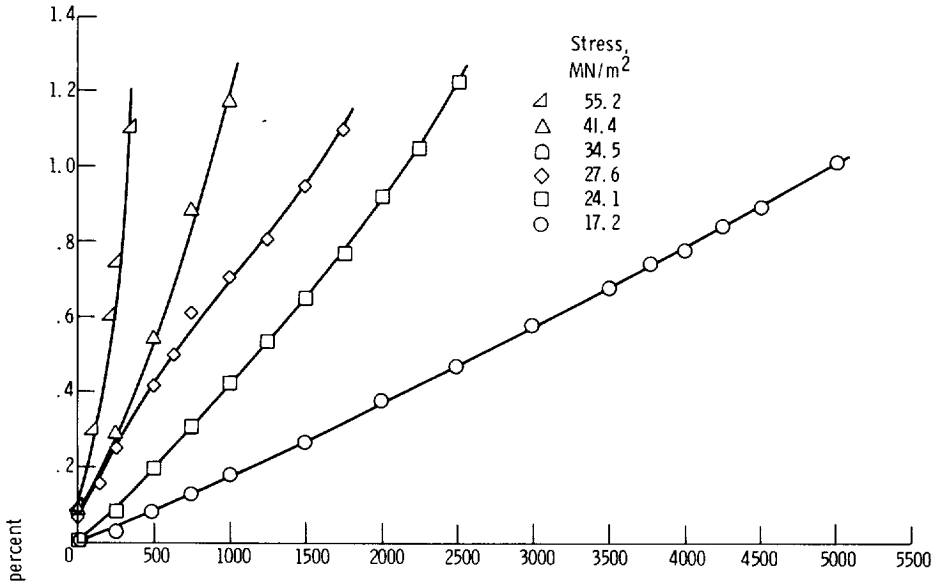

(c) 1590 K.

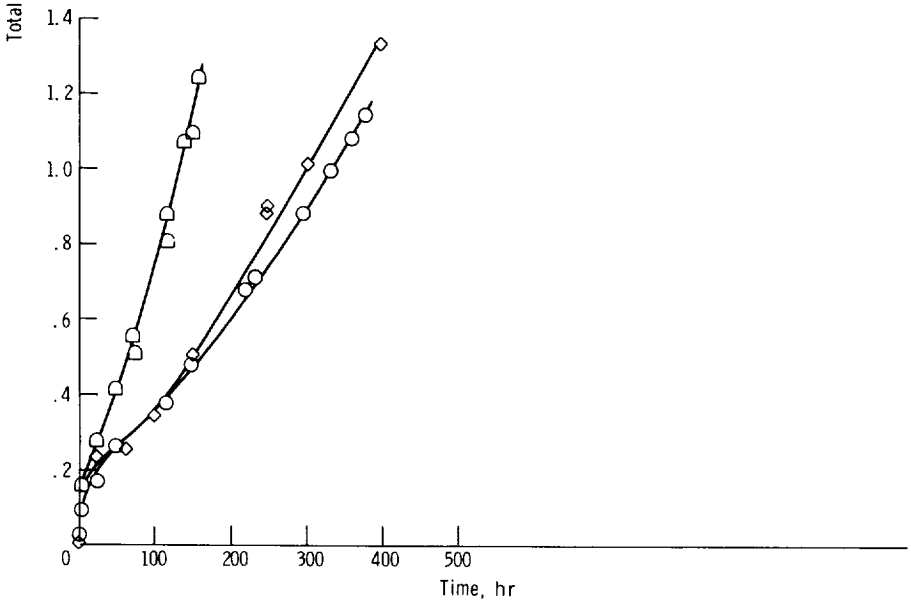

(d) 1700 K.

Figure 2. - Concluded.

$$\epsilon - \epsilon_o = (\dot{\alpha}t)^{1/2} + \dot{\epsilon}t + (\dot{\beta}t)^{3/2} \quad (1)$$

Analysis of the T-222 creep data indicated that these creep curves could also be well described by equation (1). Primary creep could be described by a time$^{1/2}$ term, secondary creep by a time term, and tertiary creep by a time$^{3/2}$ term.

This early onset of tertiary creep at strains below 1 percent for a material generally considered highly ductile is surprising. However, it is thought that this early tertiary stage of creep may be due to the continuous nucleation of voids at grain boundary ledges and precipitates. Gittins (ref. 7) observed the formation and growth of cavities at boundary ledges and precipitates during creep and has shown that the nucleation of such cavities during creep is proportional to time$^{1/2}$. Subsequent cavity growth which

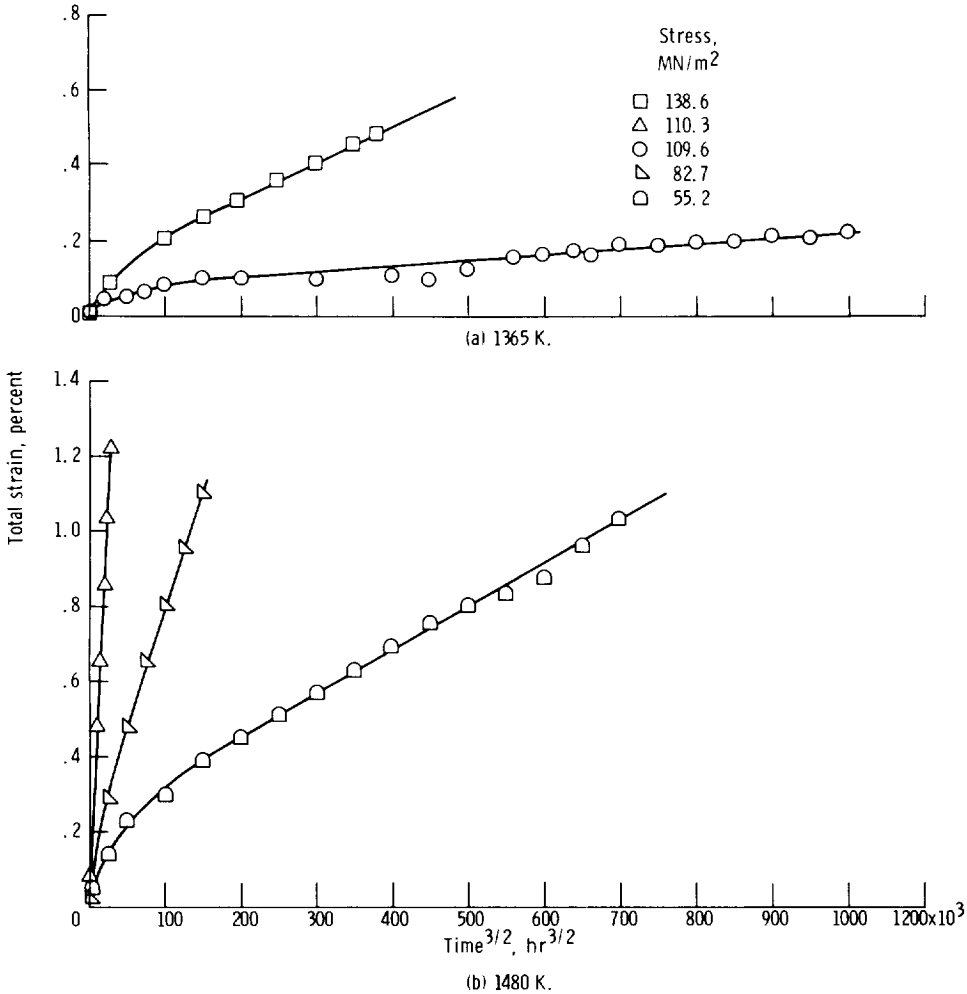

Figure 3. - Creep curves illustrating linear variation of strain with time$^{3/2}$ for T-222. Replot of data from figure 2. (Creep data from ref. 2.)

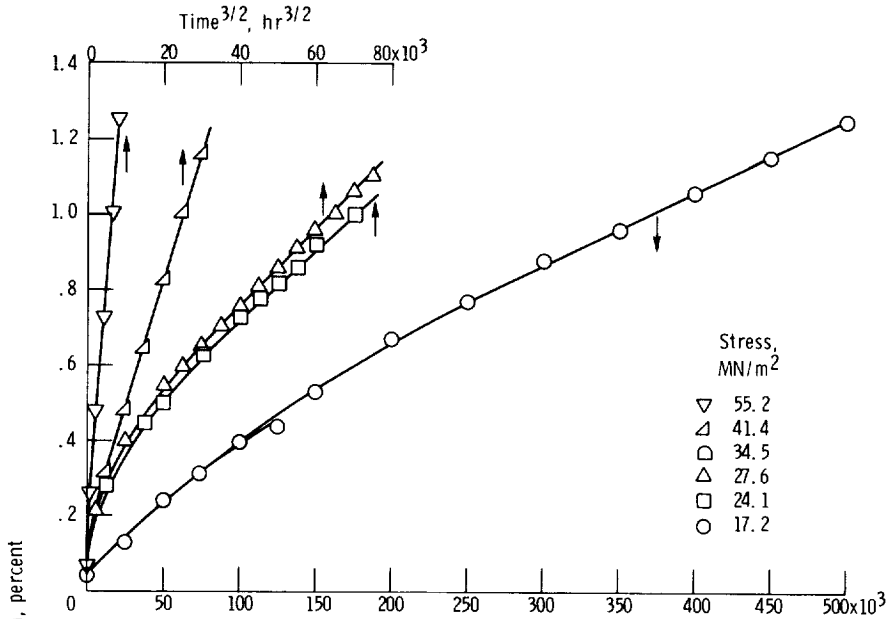

(c) 1590 K.

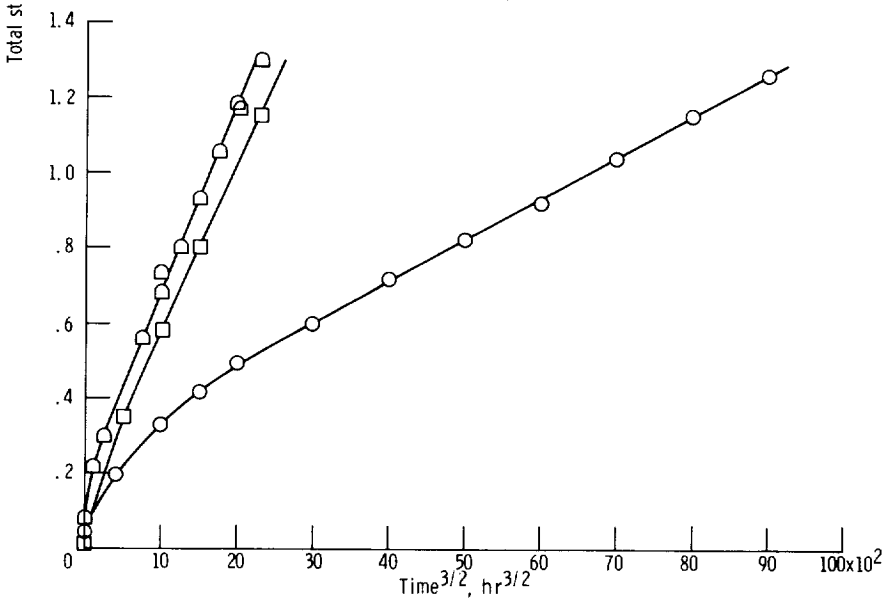

(d) 1700 K.

Figure 3. - Concluded.

TABLE II. - CREEP DATA FOR T-222 (HEAT A) ANNEALED FOR 1-HOUR AT 1810 K PRIOR TO TESTING

Specimen	Creep stress, MN/m^2	Creep temperature, K	Strain on loading, ϵ_o, percent	Tertiary creep rate, $\dot{\beta}$, $(strain^{2/3})(sec^{-1})$	Time to achieve 1-percent strain, hr	Average grain diameter, L, μm
17	138.2	1365	0.00	1.27×10^{-9}	(a)	16
1	109.6	1365	.00	3.64×10^{-10}	(b)	17
4	110.3	1480	.05	1.44×10^{-8}	840	19
3	82.7	1480	.06	4.10×10^{-9}	2620	16
2	55.2	1480	.05	1.42×10^{-9}	7550	16
5	55.2	1590	.11	3.30×10^{-8}	325	16
8	41.4	↓	.07	1.34×10^{-8}	870	16
6	27.6	↓	.07	6.13×10^{-9}	1580	15
20	24.1	↓	.23	5.44×10^{-9}	2160	16
19	17.1	↓	.01	2.01×10^{-9}	5000	16
23	34.5	1700	.00	1.75×10^{-7}	137	16
9	27.6	1700	.14	7.90×10^{-8}	300	14
18	17.2	1700	.09	2.94×10^{-8}	335	17

[a]Test terminated at 5100 hr with 0.45 percent strain.

[b]Test terminated at 10 000 hr with 0.22 percent strain.

occurs by the adsorption of vacancies from the grain boundaries is directly proportional to time. It is considered that this nucleation reaction is responsible for the $time^{3/2}$ variation of creep strain during early tertiary creep, while cavity growth becomes predominant during later creep.

With regard to intentions to generate preliminary engineering design data, mainly the stress levels for total creep strains of 1 percent in 10 000 to 50 000 hours, only the tertiary creep rates will be considered in this report. The significance of using the tertiary creep rates is illustrated in figure 3. Here, the creep curves from figure 2 are replotted to show the linear variation of strain with $time^{3/2}$. The tertiary creep rates determined from figure 3 allow for a more accurate extrapolation of creep strains to the long times of interest. The tertiary creep rates along with creep test conditions are given in table II.

Analysis of Tertiary Creep Rates

Presently no creep model exists to predict or correlate tertiary creep rate constants. However, steady-state creep models have been applied to primary creep rate

constants where creep strains vary linearly with time to the 1/2 or 1/3 (transient creep stage). Garofalo (ref. 8) points out that the stress dependency for transient creep must depend on stress in a manner similar to that for steady-state creep. Likewise, the apparent activation energies during transient and steady-state creep are similar, suggesting that the processes controlling creep are the same during these two stages. With the assumption that mode or modes of deformation operative during the long time creep of the T-222 alloy up to 1 percent total strain are constant, the kinetics and structural dependence of tertiary creep will be evaluated using steady-state creep models. Therefore, in an effort to characterize the creep data of this study such that extrapolations to longer times would more closely reflect the observed tertiary creep behavior, the normally used steady-state creep models were modified only to the extent that the tertiary creep rate constant replaces the secondary creep rate.

Stress Dependence of Creep

Analysis of the creep data presented in table II indicated that the stress dependency of the tertiary creep rate varied with the applied stress. The data could be separated into two groups. The low stress data ($\sigma < 80$ MN/m^2) exhibited a stress dependency n of 2.33 while the high stress data exhibited an n of 4.74 as shown in figure 4. Data for the Ta-10W alloy at comparable grain sizes and low stresses show an n of approximately 1.7 (ref. 1). The higher value of n for the T-222 alloy over the Ta-10W alloy may reflect carbide particle strengthening in T-222.

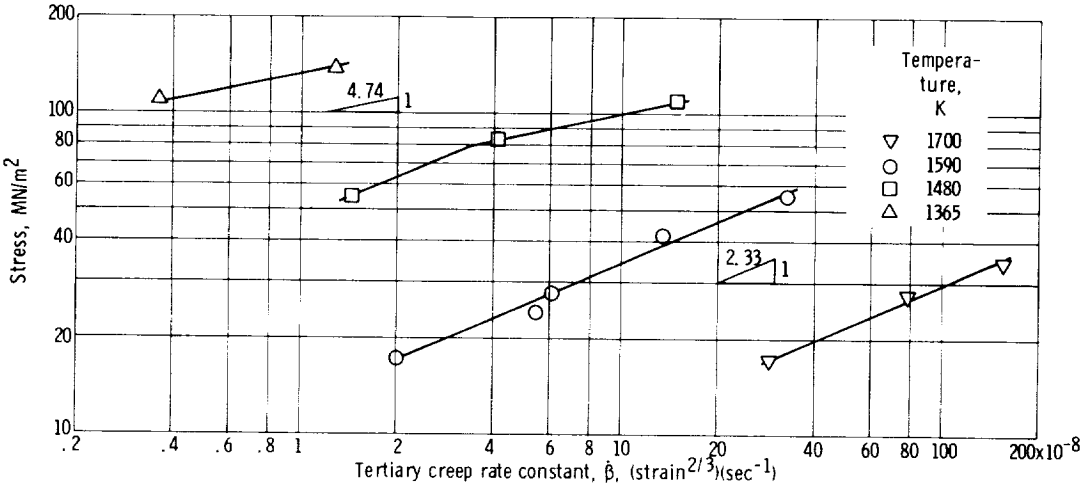

Figure 4. - Stress dependence of tertiary creep rate constant.

Temperature Dependence of Creep

During the determination of the stress dependency it was noted that the apparent activation energy for tertiary creep was constant for both high and low stress regions. The ΔH_c of 545 kJ/g-mol is significantly higher than that for self-diffusion of tantalum (approximately 420 kJ/g-mol and the previously observed ΔH_c for Ta-10W of 378 kJ/g-mol (ref. 1). This high ΔH_c is commonly associated with creep of materials strengthened by particles. Present theories of "microcreep" mechanisms (refs. 10 to 12) imply that the dislocation substructure is stabilized by particles. Thus in the case of the T-222 alloy, extensive precipitation of second-phase carbide particles during creep testing would severely impede dislocation glide and may account for the high ΔH_c

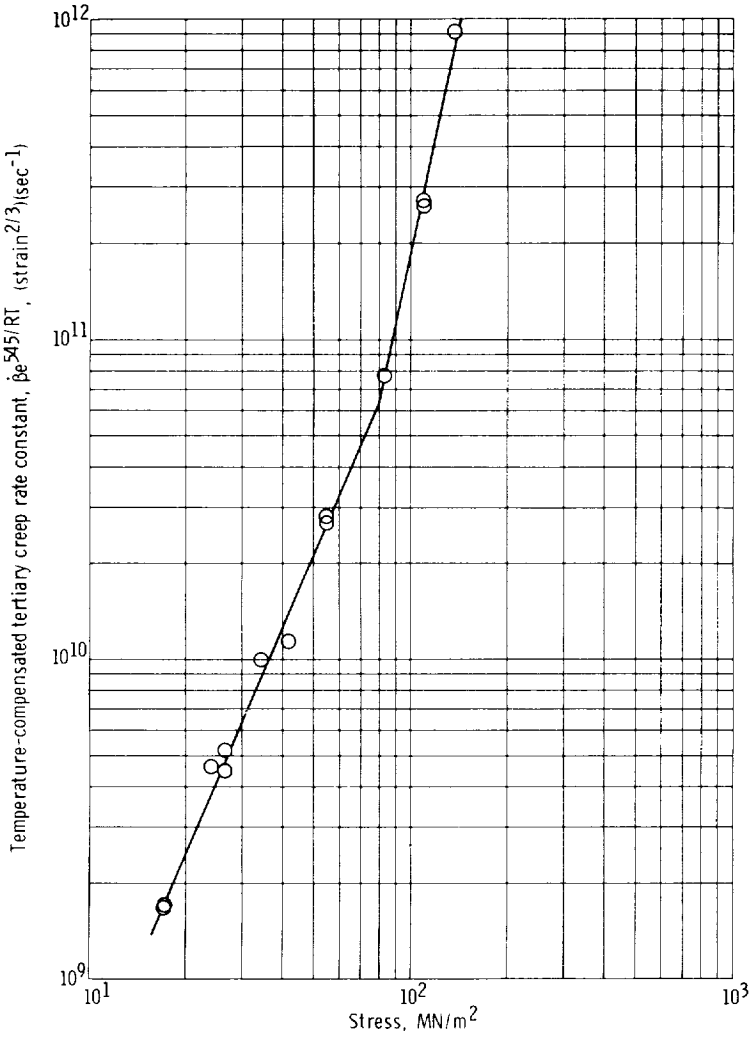

Figure 5. - Effect of stress on temperature-compensated tertiary creep rate constant for T-222 (heat A). Specimens were annealed for 1 hour at 1810 K before testing. Average grain diameter, 16 micrometers.

observed.

A plot of the temperature-compensated creep rate constant against applied stress is given in figure 5. The data show a strong likeness to Langdon's (ref. 9) model for grain boundary sliding, expressed as:

$$\dot{\epsilon}_s = \left(K\sigma^{4.5} + K' \frac{\sigma^2}{L}\right) e^{-\Delta H_c/RT} \tag{2}$$

In this model, sliding occurs by movement of dislocations along or adjacent to the boundary by a combination of glide and climb. Langdon's model predicts a creep rate proportional to σ^2 at an intermediate stress range between the low stress diffusional creep regime and the higher stress range where creep is controlled by dislocation climb. The model further proposes that the two deformation mechanisms are concurrent. The data of the present study appear to be in accord with this model and imply that "grain boundary sliding," which is accommodated by climb adjacent to the grain boundaries, predominates at low stresses while normal dislocation climb throughout the structure is rate controlling at higher stresses.

Effects of Carbide Precipitation on Creep

The effects of carbide additions on the tensile and stress rupture properties of refractory materials, especially those carbides of the reactive metals hafnium, zirconium, and titanium, are well known (refs. 13 to 17).

The study of particle hardening in tantalum alloys is complicated by the fact that they do not always display classical age-hardening behavior. Chang (ref. 13) attributes this phenomena to the less potent hardening of precipitates than dissolved interstitials and to the rapid coarsening of precipitates during aging. Ammon and Harrod (ref. 16) have also noted a lack of aging response for the T-222 alloy.

This lack of classical aging response suggests that carbon and reactive metal additions to tantalum may be ineffective creep strengtheners. However, this study and previous long-time creep studies (refs. 1, 2, and 6) show that the carbon-containing alloys are stronger and that the apparent activation energy for creep ΔH_c for $\dot{\epsilon}_s$ as well as $\dot{\beta}$ of the carbon-bearing T-222 alloy is approximately 30 percent greater than the noncarbon-containing alloys. The higher ΔH_c for T-222 suggests that precipitate-dislocation interactions do occur during creep.

It has been shown (refs. 16 and 18 to 22) that alloys in the tantalum-hafnium-carbon system, such as T-222, precipitate predominately two carbide compounds. Phase identification studies on the nominal T-222 alloy (Ta-9.6W-2.4Hf-0.01C) have identified

TABLE III. - ANALYSES OF EXTRACTED RESIDUES

FROM CREPT T-222 SPECIMENS (HEAT B)

Specimen	Duration of test, hr (a)	Total strain achieved, percent	Precipitated phase	Lattice parameter, nm
34	5	0.05	(Hf, Ta)C	45.86
33	50	.16	(Hf, Ta)C	45.90
32	140	.44	(Hf, Ta)C	46.00
31	212	.53	(Hf, Ta)C	46.00
30	502	1.50	(Hf, Ta)C	46.00
17	932	2.1	{(Hf, Ta)C, Ta_2O_5}	[b]45.94

[a]Specimens were annealed for 1 hr at 2255 K and creep tested at 1590 K and 82.7 MN/m^2 for indicated times.

[b]The low lattice parameter may be due to the presence of oxygen. Test 17 was the only condition in which a very weak indication of an oxide were noted.

these carbides as the hcp dimetal carbide $(Ta, Hf)_2C$, containing about 10 percent hafnium in solution with tantalum and the fcc monocarbide (Ta, Hf)C, consisting of a solid solution of HfC and TaC.

To identify the particles responsible for the enhanced creep strength in the T-222 alloy, a series of time-interrupted creep tests were conducted on 2255 K solution-annealed material. Creep tests were performed at 1590 K under a stress of 82.7 MN/m^2 for various periods of time, nominally 5, 50, 150, 200, 500, and 1000 hours. The actual times and total strains achieved along with particle lattice parameters are given in table III. The more significant data obtained from these tests were that only the fcc monocarbide phase (Hf, Ta)C was detected and the lattice parameters indicated a change in composition with time. The lattice parameter changes correspond to a change from 21 mole percent TaC (a_0 = 45.86 nanometers) to 15 mole percent TaC (a_0 = 46.00 nanometers), the apparent equilibrium composition for (Hf, Ta)C (ref. 23).

Metallographic studies also showed an extensive interaction of particles with dislocations and grain boundaries. Figure 6 shows the microstructure of a cathodically etched specimen which had been strained to 2.1 percent. Figure 6(a) shows that extensive precipitation of (Hf, Ta)C has taken place at the grain and subgrain boundaries. Figures 6(b) and (c) show that the particles have been dragged by the migrating grain boundaries. Assuming that particle motion is diffusion-controlled as proposed by Ashby (ref. 24), that is, grain boundary dislocation absorbing vacancies at the lead point of a particle and emitting vacancies at the back of the particle, the particle moves forward by a Burger's vector for each sweep of a dislocation over the particle surface. Such a

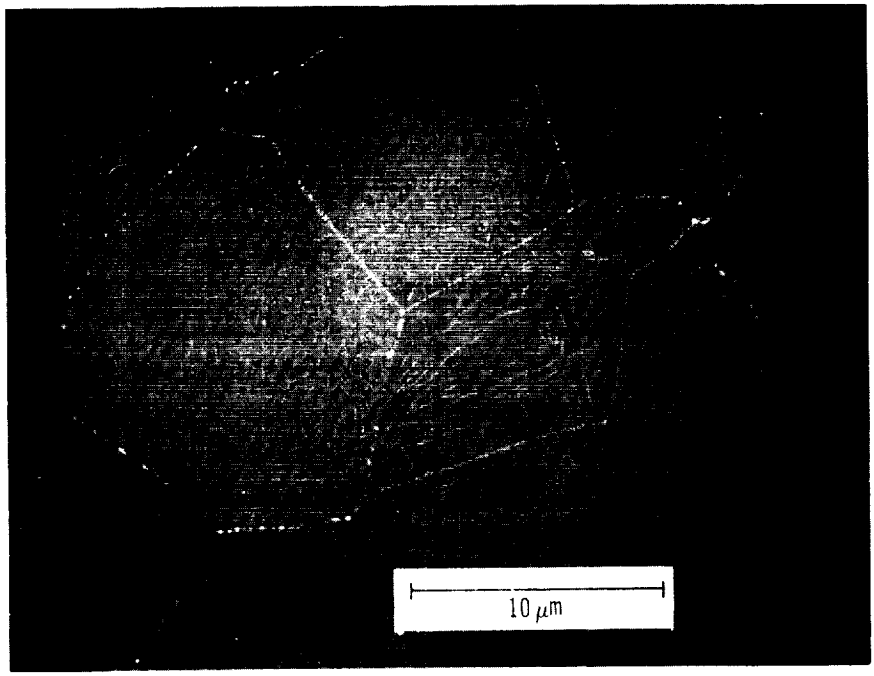

(a) Scanning electronmicrograph showing the extensive precipitation that has taken place during creep testing which delineates the grain boundaries and substructure.

Figure 6. - Photomicrographs of solution annealed (1 hr at 2255 K) T-222 alloy creep tested at 1590 K and 82.7 MN/m^2. 2.1 Percent total strain occurred in 932 hours.

(b) Transmission micrograph of carbon replica of specimen showing in greater detail the grain boundary precipitates. Note void and trail associated with precipitates which is probably due to grain boundary sliding and migration.

Figure 6. - Continued.

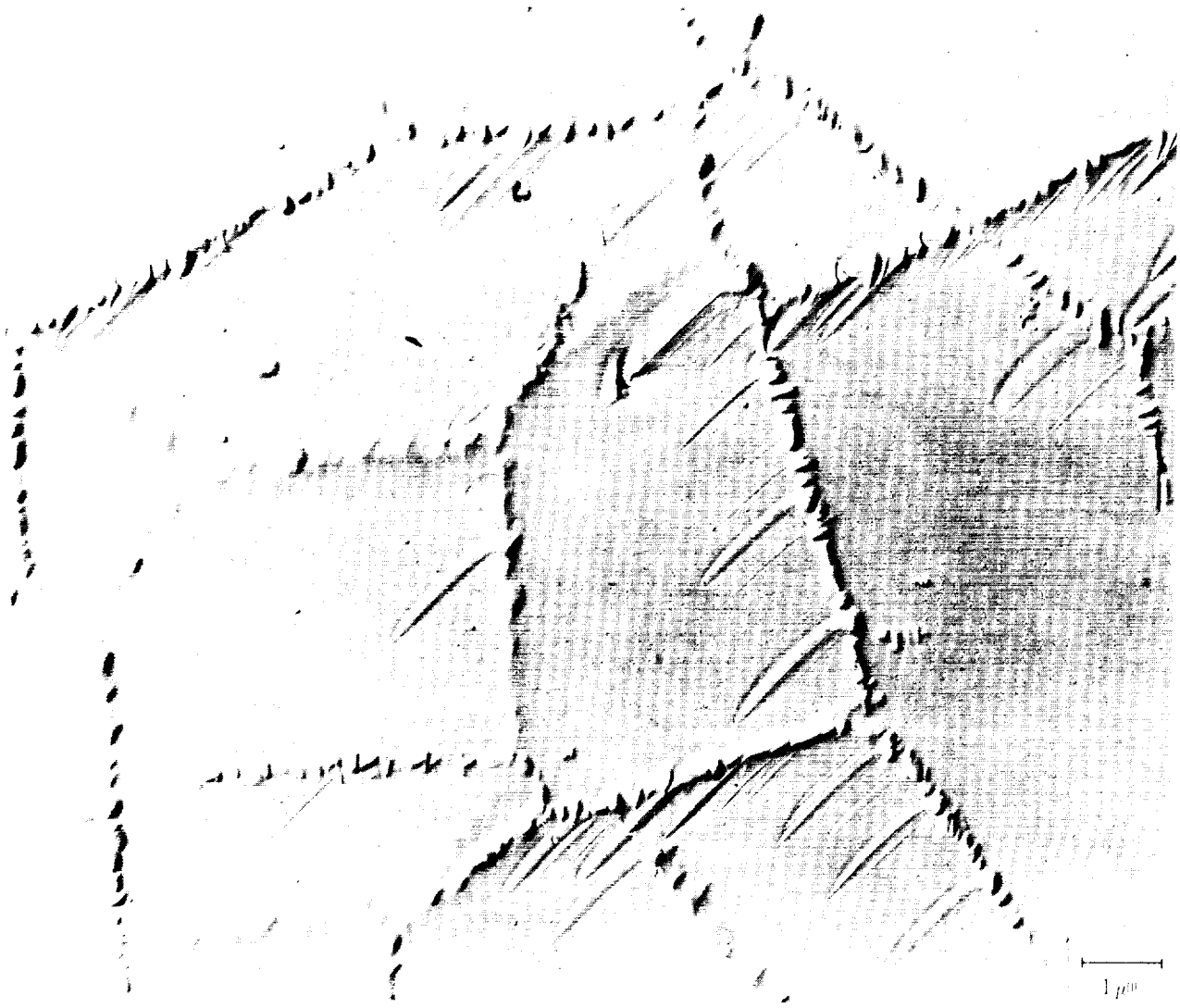

(c) Transmission micrograph of carbon replica of specimen showing precipitate dislocation interaction in creep tested T-222 delineating substructure.

Figure 6. - Concluded.

mechanism would account for the particle void trails observed in crept T-222.

The total absence of the hcp dimetal carbide from the solution annealed and crept T-222 was not expected. The data suggest that if the dimetal carbide were present initially, as would be expected following a normal aging heat treatment, it is not stable in the presence of a strain and may not affect the creep behavior. Therefore, a series of creep tests was conducted to determine the effect of classical thermal aging upon the creep strength of T-222 and to determine the effect of strain on carbide particle formation.

Creep specimens of T-222 (heat B) were vacuum annealed for 1 hour at 2255 K to dissolve all carbides and furnace cooled prior to aging or creep testing. Furnace cooling was equivalent to a temperature drop to 1300 K in approximately 5 minutes. Figure 7 is a photomicrograph of the solution-annealed microstructure and shows the relatively clean structure obtained. Thermal aging of the specimen for 310 hours at 1480 K resulted in extensive matrix and grain boundary precipitation as shown in figure 8. X-ray analysis of the bromide-extracted particles revealed the presence of only $(Ta, Hf)_2C$.

The effects of thermal aging on creep strength were investigated by creep testing two series of specimens, each respectively aged at 1300, 1365, 1480, and 1590 K for 20 and 100 hours. Figure 9(a) shows the creep curves for the 20-hour aged series and figure 9(b) for the 100-hour aged series, tested at 1480 K under a stress of 172.4 MN/m^2. The creep curves clearly show that thermal aging of T-222 prior to creep testing results in increased creep strength, and that the highest aging temperature investigated resulted in the most creep resistant structure. Figure 10 shows the change in tertiary creep rate constant with aging temperature. Table IV lists the tertiary creep rates along with the duration of test, total strain achieved, and the identified carbide phase.

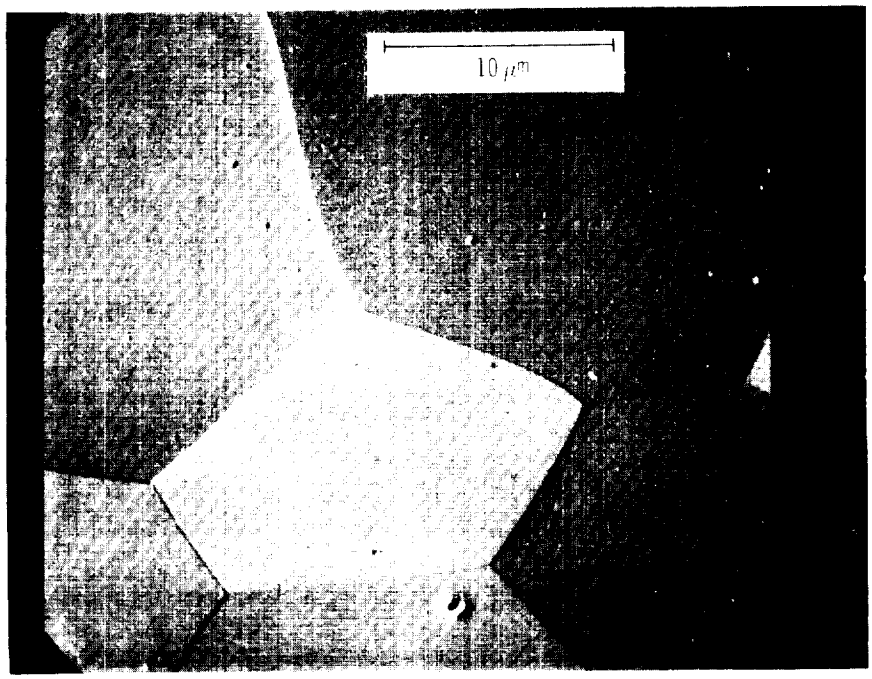

(a) Scanning electron micrograph showing relatively precipitate free microstructure obtained by furnace cooling. X300.

Figure 7. - Photomicrographs of solution annealed (1 hr at 2255 K) T-222 alloy prior to aging or creep testing.

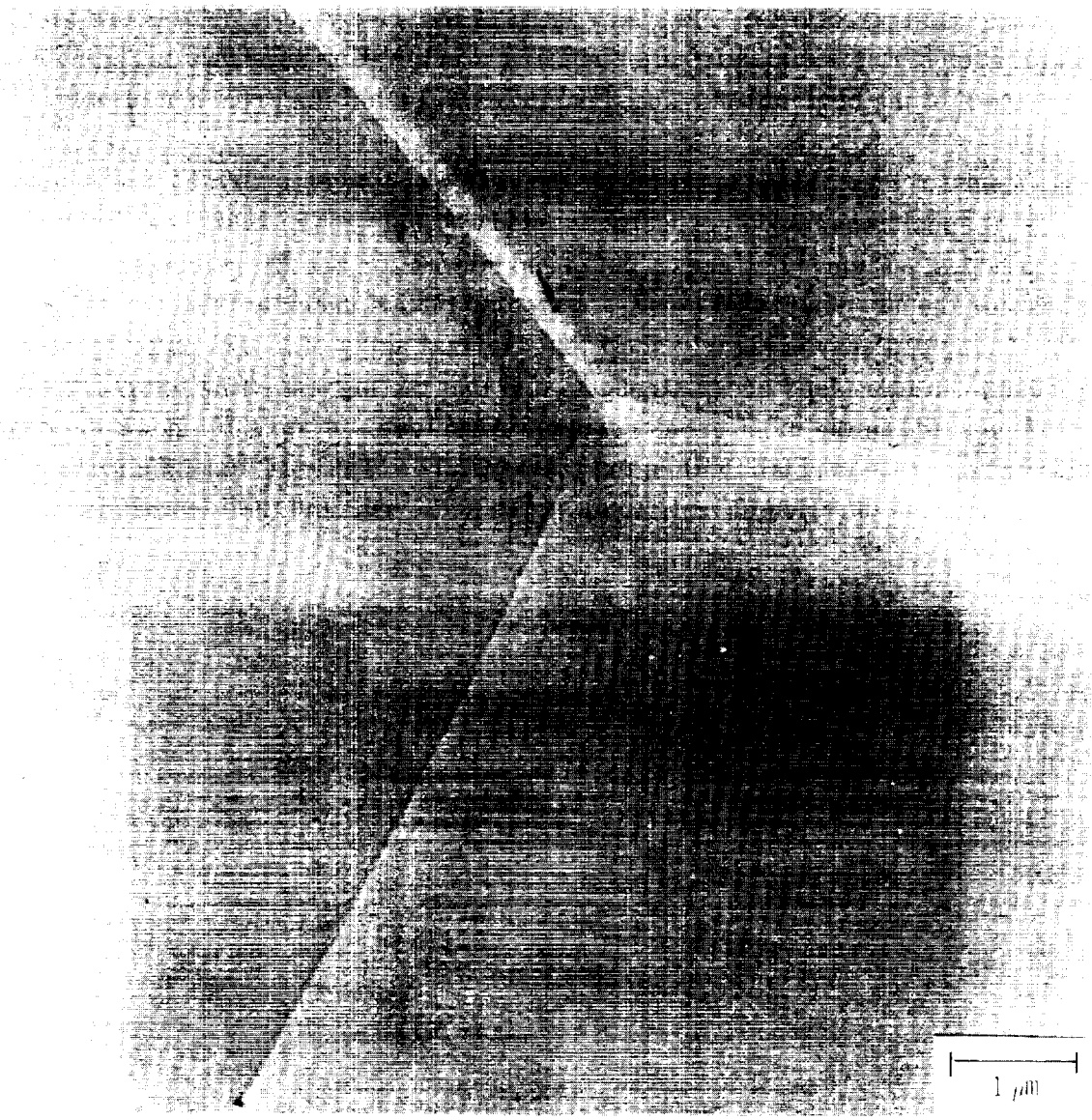

(b) Transmission micrograph of carbon replica of T-222 surface showing in greater detail the absence of matrix or grain boundary precipitates and substructure.

Figure 7. - Concluded.

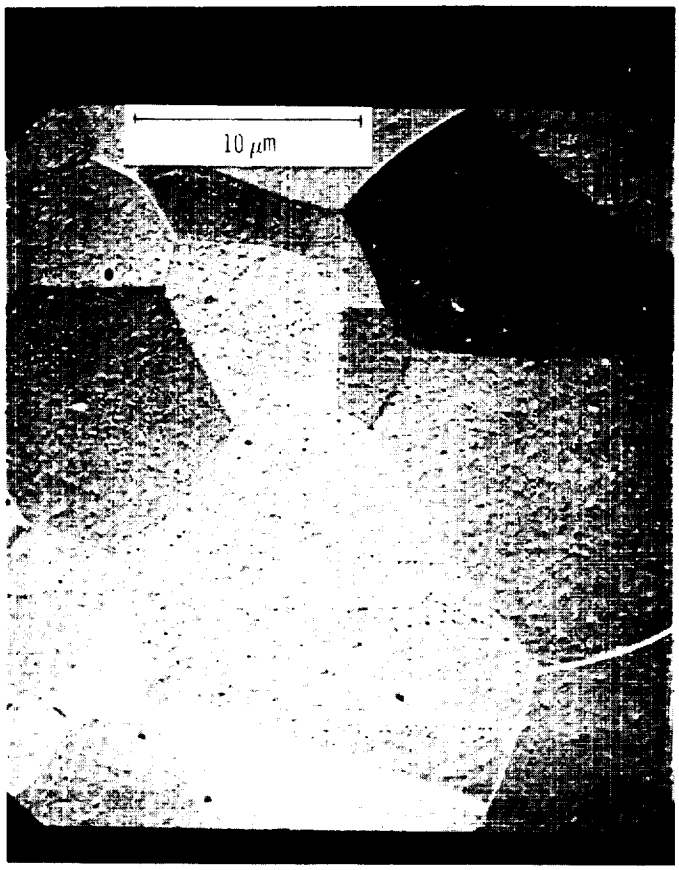

(a) Scanning electronmicrograph showing the extensive precipitation of $(Ta, Hf)_2 C$ in matrix and grain boundary. Grain boundary migration is also evident. X300.

Figure 8. - Photomicrographs of solution annealed (1 hr at 2255 K) T-222 alloy thermally aged 310 hours at 1480 K.

(b) Transmission micrograph of carbon replica of surface showing in greater detail the precipitation of $(Ta, Hf)_2 C$.

Figure 8. - Concluded.

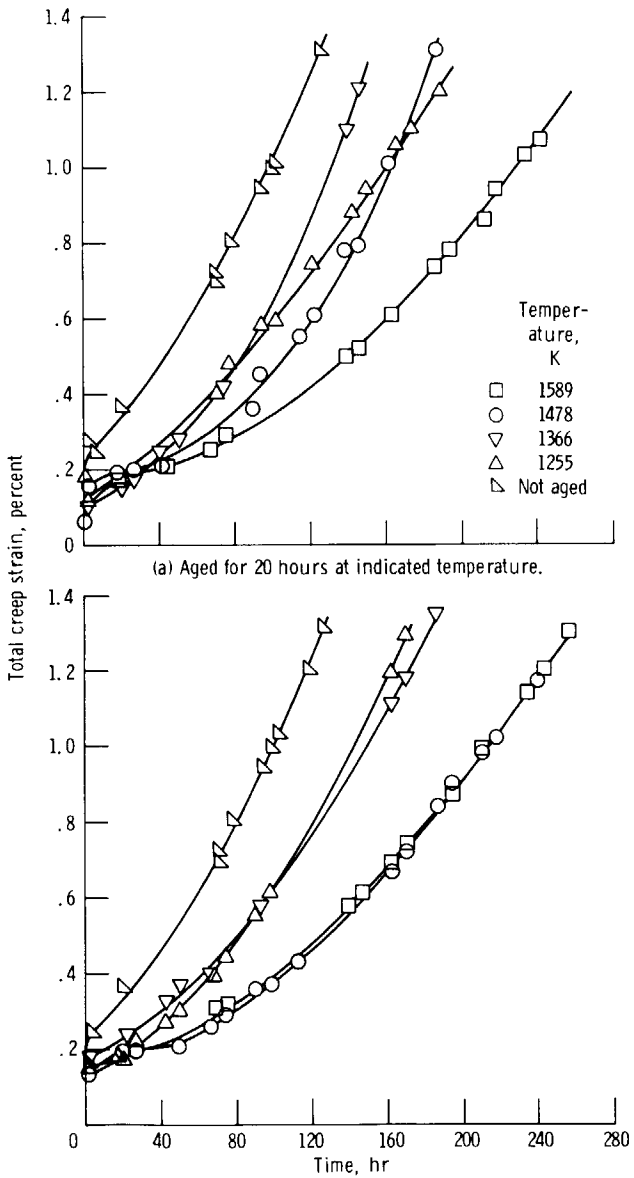

(a) Aged for 20 hours at indicated temperature.

(b) Aged for 100 hours at indicated temperature.

Figure 9. - Creep curves for T-222 (heat B) tested at 1478 K and 172.4 MN/m^2. Material was annealed for 1 hour at 2255 K and aged prior to creep testing. In all cases thermal aging shows an increase in creep strength.

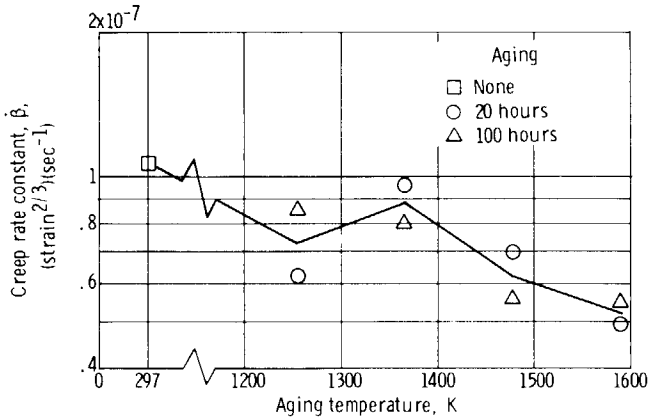

Figure 10. - Variation of creep rate constant $\dot{\beta}$ with aging temperature for T-222 (heat B). Solution annealed for 1 hour at 2255 K prior to aging. Creep tested at 1480 K and 172.4 MN/m^2.

TABLE IV. - CREEP DATA FOR SOLUTION ANNEALED AND AGED T-222 (HEAT B)

Specimen	Aging conditions[a]		Tertiary creep rate, $\dot{\beta}$, $(\text{strain}^{2/3})(\text{sec}^{-1})$[b]	Duration of test, hr	Total strain achieved, percent	Precipitated phase[c]
	Time, hr	Temperature, K				
18	---	----	1.06×10^{-7}	240	3.19	(Hf, Ta)C
26	20	1590	4.94×10^{-8}	334	1.74	(Hf, Ta)C
22	100	1590	5.46	308	1.72	--------
25	20	1480	6.97	195	1.41	(Hf, Ta)C
21	100	1480	5.51	361	2.66	--------
24	20	1365	9.60	190	1.78	(Hf, Ta)C
20	100	1365	8.04	355	4.30	--------
23	20	1255	6.19	310	2.14	$(Hf, Ta)_2C$ + (Hf, Ta)C
19	100	1255	8.50	331	3.44	$(Hf, Ta)_2C$ + (Hf, Ta)C

[a]Solution annealed for 1 hr at 2255 K prior to aging at indicated conditions.
[b]Creep testing performed at 1480 K and 172.4 MN/m^2.
[c]Precipitated phases identified by X-ray emission analyses of bromine extracted residue.

From metallographic and X-ray data, thermal aging appears to have resulted in the stabilization of boundaries and subboundaries by the presence of carbide particles. However, X-ray analysis of the bromine extractions from selected specimens (see table IV) indicates that (Hf, Ta)C is generally the predominate phase. The $(Hf, Ta)_2C$ phase was found only in the lowest temperature aged specimen and probably reflects incomplete conversion of the $(Hf, Ta)_2C$ phase present prior to creep testing. These data thus indicate that aging in the presence of strain, such as during a creep test, promotes conversion of the $(Hf, Ta)_2C$ phase to the (Hf, Ta)C phase.

Effects of Grain Size on Creep of T-222

The effect of grain size on the creep strength of T-222 is shown in figures 11 and 12 and given in table V for T-222 (heat B) tested at 1480 K under a stress of 82.7 MN/m^2.

The behavior is similar to that noted for Ta-10W (ref. 1), the creep rate decreasing with increasing grain size. The variation of the tertiary creep rate constant with grain size strongly suggests that grain boundary sliding is the major deformation mode at fine grain sizes. However, grain boundary sliding becomes less important as the grain boundary area decreases (increasing grain size) where deformation apparently changes from localized accommodation near the grain boundaries to a more uniform distribution throughout the entire structure.

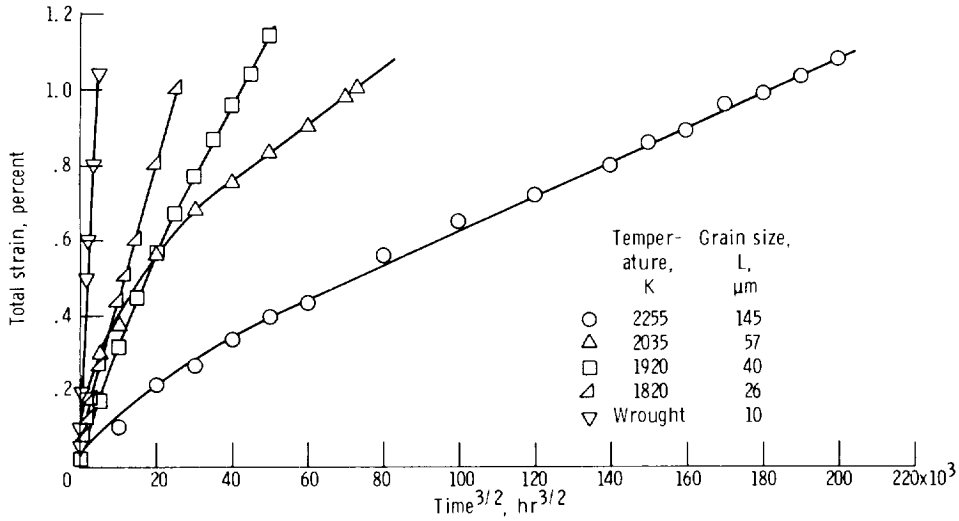

Figure 11. - Influence of grain diameter on creep behavior of T-222 (heat B) at 1480 K and 82.7 MN/m^2. All specimens annealed for 1 hour at indicated temperatures with average grain diameters indicated.

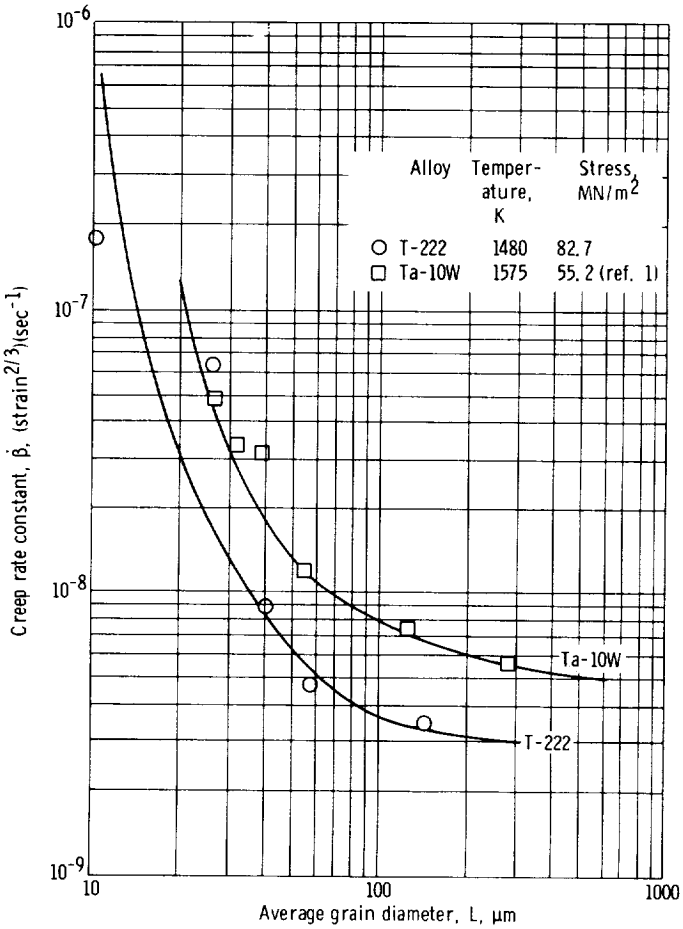

Figure 12. - Variation of creep rate constant $\dot{\beta}$ with average grain diameter L for T-222 and Ta-10W alloy.

TABLE V. - EFFECT OF ANNEALING TEMPERATURE ON GRAIN SIZE AND CREEP OF T-222 (HEAT B) AT 1480 K AND 82.7 MN/m^2

Specimen	1-Hour annealing temperature, K	Average grain diameter, L, μm	Tertiary creep rate, $\dot{\beta}$, $(strain^{2/3})(sec^{-1})$	Time to achieve 1-percent strain, hr
7	(a)	10	1.76×10^{-7}	18
1	1810	26	6.33×10^{-8}	120
3	1920	40	9.12×10^{-9}	1200
10	2030	57	4.82×10^{-9}	1700
--	2140	75	Not tested	----
6	2255	145	3.50×10^{-9}	3200

[a]Annealed by manufacturer for 2 hr at 1755 K.

Mechanism of Creep

The long time creep behavior of T-222 at temperatures in the 0.3 to 0.6 T_m regime is complex. Two or more modes of deformation are apparently operative. There is evidence of dissolution and strain induced precipitation of carbide particles, grain boundary migration, and dislocation-vacancy-precipitate interactions taking place during creep of tantalum T-222. The change of the stress dependency of the tertiary creep rate constant with applied stress and the high apparent activation energy for tertiary creep suggests that creep deformation is controlled by a combination of dislocation glide and climb with grain boundary sliding operating independently and concurrently.

The data of the present study thus implies that grain boundary sliding, which is accommodated by dislocation climb adjacent to and along the grain boundaries, predominates at low stresses, while normal dislocation glide and climb is rate controlling at higher stresses.

CONCLUDING REMARKS

Annealed polycrystalline T-222 exhibits long-time creep behavior similar to Ta-10W, with creep strength increasing with increasing grain size. The major portion of the creep curves could be best described by a tertiary creep rate, strain varying linearly with time$^{3/2}$, at total strains well below 1 percent. Based on the assumption that the basic modes of deformation during creep testing to total strains of 1 percent are similar during both secondary and tertiary creep, stress and temperature dependencies were determined for the observed tertiary creep rates. This treatment allows the engineering design data sought to be readily calculated.

In figure 13, a plot is presented of the creep strength for 1 percent creep strain in 10 000 hours at the temperatures of interest for fine grained T-222 and Ta-10W. At 1365 K for T-222, this stress is 94.5 MN/m^2 and for Ta-10W is 23.2 MN/m^2. At higher temperatures, the strength for both materials decreases rapidly. For example, these values for T-222 are 20 MN/m^2 at 1480 K, 5.3 MN/m^2 at 1590 K, and 1.7 MN/m^2 at 1700 K. The strength of T-222 appears to be approximately four times greater than that of the Ta-10W alloy. On the basis of the observed creep behavior, the T-222 alloy appears not to be suitable for the containment of liquid alkali-metals in lightweight systems at temperatures above approximately 1500 K.

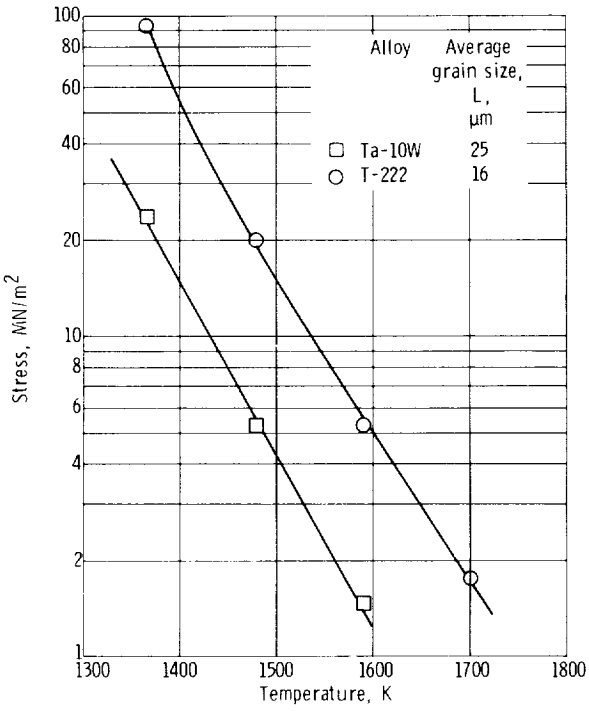

Figure 13. - Effect of temperature on allowable stress level required to limit total creep strain to 1 percent in 10 000 hours. Extrapolation based on observed tertiary creep rates $\dot{\beta}$.

SUMMARY OF RESULTS

The results of this study of the kinetics and structural dependence of the long-time, high vacuum, high temperature, creep behavior of the tantalum T-222 alloy are:

1. The T-222 alloy exhibits grain size effects and an early onset of tertiary creep, similar to the behavior of the Ta-10W alloy. The creep strength advantage of T-222 over Ta-10W, approximately a factor of four, is attributed to particle strengthening by a mixed fcc monocarbide, (Hf, Ta)C.

2. The apparent activation energy for tertiary creep, 545 kJ/g-mol, for T-222, is substantially higher than the 378 kJ/g-mol observed for Ta-10W and is also attributed to carbide particle strengthening.

5. Grain boundary voids are formed adjacent to carbide particles. Void trails are observed adjacent to those particles which appear to be moving with migrating boundaries. This void formation may account for the observation of tertiary creep at strains of less than 1 percent.

4. Thermal aging of the T-222 to produce the hcp dimetal carbide $(Hf, Ta)_2C$ prior to creep testing enhances the creep strength.

5. The fcc monocarbide (Hf, Ta)C is the stable particle during creep testing. The $(Hf, Ta)_2C$ produced by thermal aging converts to (Hf, Ta)C during creep straining.

Lewis Research Center,
National Aeronautics and Space Administration,
Cleveland, Ohio, January 30, 1974,
501-21.

APPENDIX - CONVERSION OF THE INTERNATIONAL SYSTEM OF UNITS TO U. S. CUSTOMARY UNITS

The International System of Units (SI) was adopted by the Eleventh General Conference of Weights and Measures in Paris in October 1960. Conversion factors for the units used in this report are derived from values in reference 25 and are presented in the following table:

Quantity	SI unit	Conversion factor (a)	U. S. customary unit
Pressure	newton/meter^2 (N/m^2)	7.501×10^{-3}	mm of mercury
Force	newton (N)	0.2248	lbf
Length	meter (m)	39.37	in.
Stress	newton/meter^2 (N/m^2)	1.45×10^{-7}	ksi = 1000 lbf/in.^{2}
Temperature	kelvin (K)	$^{\circ}F = \frac{9}{5}(K - 255.4)$	degree Fahrenheit ($^{\circ}F$)

[a]Multiply value given in SI units by conversion factor to obtain equivalent value in U. S. customary units or apply conversion formula.

The following prefixes are used to indicate multiples of SI units:

Prefix	Factor by which unit is multiplied
nano (n)	10^{-9}
micro (μ)	10^{-6}
milli (m)	10^{-3}
kilo (k)	10^{3}
mega (M)	10^{6}

REFERENCES

1. Titran, Robert H.; and Klopp, William D.: Long Time Creep Behavior of Tantalum - 10 Tungsten in High Vacuum. NASA TN D-6044, 1970.

2. Titran, Robert H.: Creep of Tantalum T-222 Alloy in Ultrahigh Vacuum for Times up to 10,000 Hours. NASA TN D-4605, 1968.

3. Titran, Robert H.; and Hall, Robert W.: High-Temperature Creep Behavior of a Columbium Alloy, FS-85. NASA TN D-2885, 1965.

4. Titran, Robert H.; and Hall, Robert W.: Ultrahigh-Vacuum Creep Behavior of Columbium and Tantalum Alloys at 2000° and 2200° F for Times Greater than 1000 Hours. Vol. 2 of Refractory Metals and Alloys IV - Research and Development, R. I. Jaffee, G. M. Ault, J. Maltz, and M. Semchyshen, eds., Gordon and Breach Science Publ., 1967, pp. 761-774.

5. Stephenson, R. L.: Creep-Rupture Properties of Unalloyed Tantalum, Ta-10%W and T-111 Alloys. ORNL-TM-1994, Oak Ridge National Laboratory, Dec. 1967.

6. Sheffler, K. D.; Sawyer, J. C.; and Steigerwald, E. A.: Mechanical Behavior of Tantalum-Base T-111 Alloy at Elevated Temperature. Trans. ASM, vol. 62, no. 3, Sept. 1969, pp. 749-758.

7. Gittins, A.: The Mechanism of Cavitation in Copper During Creep. Metal Science Journal, vol. 1, 1967, pp. 214-216.

8. Garofalo, Frank: Fundamentals of Creep and Creep-Rupture in Metals. Macmillan Company, 1965, pp. 91 and 156.

9. Langdon, Terence G.: Grain Boundary Sliding as a Deformation Mechanism During Creep. Phil. Mag. vol. 22, no. 178, Oct. 1970, pp. 689-700.

10. Weertman, J.: Creep of Indium, Lead, and Some of Their Alloys with Various Metals. Trans. AIME, vol. 218, no. 2, Apr. 1960, pp. 207-218.

11. Conrad, H.; Bernet, E.; and White, J.: Correlation and Interpretation of High Temperature Mechanical Properties of Certain Superalloys. Joint International Conference on Creep. Inst. Mech. Eng., 1963, pp. 1-9 to 1-15.

12. Garofalo, Frank: Fundamentals of Creep and Creep-Rupture in Metals. Macmillan Company, 1965, p. 193.

13. Chang, W. H.: Effect of Carbide Dispersion in Tantalum-Base Alloys. Vol. 1 of Refractory Metals and Alloys IV - Research and Development, R. I. Jaffe, G. M. Ault, J. Maltz, and M. Semchyshen, eds., Gordon and Breach Science Publ., 1967, pp. 405-422.

14. Raffo, P. L.; and Klopp, W. D.: Solid Solution and Carbide Strengthened Arc-Melted Tungsten Alloys. Vol. 1 of Refractory Metals and Alloys IV - Research and Development, R. I. Jaffe, G. M. Ault, J. Maltz, and M. Semchyshen, eds., Gordon and Breach Science Publ., 1967, pp. 501-518.

15. White, J. E.; and Barr, R. Q.: Dispersion Strengthened Molybdenum and Molybdenum-Base Alloys. Vol. 1 of Refractory Metals and Alloys IV - Research and Development, R. I. Jaffe, G. M. Ault, J. Maltz, and M. Semchyshen, eds., Gordon and Breach Science Publ., 1967, pp. 541-555.

16. Ammon, R. L.; and Harrod, D. L.: Strengthening Effects in Ta-W-Hf Alloys. Vol. 1 of Refractory Metals and Alloys IV - Research and Development, R. I. Jaffe, G. M. Ault, J. Maltz, and M. Semchyshen, eds., Gordon and Breach Science Publ., 1967, pp. 423-442.

17. Klopp, W. D.; Raffo, P. L.; and Witzke, W. R.: Strengthening of Molybdenum and Tungsten Alloys with HfC. Jour. Metals, vol. 23, no. 6, June 1971, pp. 27-38.

18. Buckman, R. W., Jr.; and Goodspeed, R. C.: Considerations in the Development of Tantalum Base Alloys. Refractory Metal Alloys: Metallurgy and Technology. I. Machlin, R. T. Begley, and E. D. Weisert, eds., Plenum Press, 1968, pp. 373-394.

19. Buckman, R. W., Jr.; and Goodspeed, R. C.: Precipitation Strengthened Tantalum Base Alloys. NASA CR-1642, 1971.

20. Rudy, E.: Ternary Phase Equilibra in Transition Metal-Boron-Carbon-Silicon Systems. Part II: Ternary Systems. Vol. 1: Ta-Hf-C System. ARML-TR-65-2, Part 2, vol. 1, Aerojet General Corp. (AD-470827), June 1965.

21. Filippi, A. M.: Production and Quality Evaluation of T-222 Tantalum Alloy Sheet. Final Report, WANL-PR-(KK)-003 Westinghouse Astronuclear Laboratory (AD-837296), Jan. 1968.

22. Buckman, R. W., Jr.; and Begley, R. R.: Development of High Strength Tantalum Base Alloys. Recent Advances in Refractory Alloys for Space Power Systems, NASA SP-245, 1969, pp. 19-38.

23. Nowotny, H.; Kieffer, R.; Benesovsky, F.; Brukl, C.; and Rudy, E.: The Partial Systems of HfC with TiC, ZrC, VC, NbC, TaC, Cr_3C_2, Mo_2C (MoC), WC, and UC. Monatshefte fuer Chemie, Vol. 90, 1959, pp. 669-679.

24. Ashby, M. F.: Boundary Defects and the Mechanism of Particle Movement Through Crystals. Scripta Met., vol. 3, pp. 843-848, 1969.

25. Mechtly, E. A.: The International System of Units, Physical Constants and Conversion Factors, Revised. NASA SP-7012, 1969.

"The aeronautical and space activities of the United States shall be conducted so as to contribute . . . to the expansion of human knowledge of phenomena in the atmosphere and space. The Administration shall provide for the widest practicable and appropriate dissemination of information concerning its activities and the results thereof."

—NATIONAL AERONAUTICS AND SPACE ACT OF 1958

NASA SCIENTIFIC AND TECHNICAL PUBLICATIONS

TECHNICAL REPORTS: Scientific and technical information considered important, complete, and a lasting contribution to existing knowledge.

TECHNICAL NOTES: Information less broad in scope but nevertheless of importance as a contribution to existing knowledge.

TECHNICAL MEMORANDUMS: Information receiving limited distribution because of preliminary data, security classification, or other reasons. Also includes conference proceedings with either limited or unlimited distribution.

CONTRACTOR REPORTS: Scientific and technical information generated under a NASA contract or grant and considered an important contribution to existing knowledge.

TECHNICAL TRANSLATIONS: Information published in a foreign language considered to merit NASA distribution in English.

SPECIAL PUBLICATIONS: Information derived from or of value to NASA activities. Publications include final reports of major projects, monographs, data compilations, handbooks, sourcebooks, and special bibliographies.

TECHNOLOGY UTILIZATION PUBLICATIONS: Information on technology used by NASA that may be of particular interest in commercial and other non-aerospace applications. Publications include Tech Briefs, Technology Utilization Reports and Technology Surveys.

Details on the availability of these publications may be obtained from:

SCIENTIFIC AND TECHNICAL INFORMATION OFFICE

NATIONAL AERONAUTICS AND SPACE ADMINISTRATION

Washington, D.C. 20546